Natural vs Artificial Face Classification using Uniform Local Directional Patterns and Wavelet Uniform Local Directional Patterns

Darryl D'Souza and Roman V. Yampolskiy
Computer Engineering and Computer Science
J.B. Speed School of Engineering, University of Louisville, Louisville, Kentucky 40292
Email: darryl.dsouza@louisville.edu, roman.yampolskiy@louisville.edu

***Abstract*—Face classification is a technique used in Biometrics to help distinguish between facial images. However, this technique has been applicable on human face images only. Online virtual worlds such as Second Life, Sims Online, etc. are gaining popularity over the Internet. They require human users to create a digital persona of oneself, known as an "avatar". Several avatars are designed to resemble human users. With crime being reported in virtual worlds, computer-generated avatar faces being created from human faces and human-resembling humanoids being designed, there is a need to distinguish between natural and artificial faces. Our work applies two new face classification techniques on grayscale, facial images of humans and avatars to tell them apart. (1) Uniform Local Directional Pattern (ULDP) utilizes the uniform patterns from Local Directional Pattern (LDP) (2) Wavelet Uniform Local Directional Pattern (WULDP) applies the ULDP technique on the wavelet transform of an image. Extensive experiments conducted on five different face image datasets (Caltech, FERET for human faces and Entropia, Second Life, Evolver for avatar faces) achieve baseline average classification accuracies of 98.55% using ULDP and 89.55% using WULDP respectively.**

***Keywords*-Avatars; Virtual worlds; Second Life; Local Directional Patterns (LDP); Wavelet Transforms; Gaussian noise;**

I. Introduction

Face classification is a technique that segregates facial images into different groups based on criteria such as age [1], [2], gender [3], [4] and facial expressions [5]. It is widely used in several biometric application domains such as access control, surveillance, identification systems, etc. The process can be divided into two stages. The first stage employs a feature extractor to select the significant feature and the second uses a classifier to assign class labels to a new face image based on these extracted features [6]. However, here we deal with human face images in the native domain only. With advanced technologies one can virtually model the human body, especially the face, by creating a digital persona of oneself known as an *avatar*. Virtual reality is being gradually linked to physical reality with several designed avatars resembling their creators. Online Virtual Worlds (VW) such as Second Life, Sims Online, etc. are gaining popularity wherein human users create avatars representing themselves. VW have been used constructively for the benefit of the society. However, there are safety and security concerns as well e.g. cyberterrorism activities and economic crimes such as money laundering [7]. As the physical and virtual worlds come closer, the distinction between the two begins to fade, calling for security systems capable of working in the contexts of physical and virtual reality [8]. Thus, existing biometric authentication schemes must be extended into the virtual domain [9], [10] to generate a digital footprint of the human user. Moreover, computer-generated virtual avatars are also used to simulate human emotions [11] and communicate/chat with users [12]. So how does one measure how realistic these avatars are based on their face images? Figure 1 shows examples of remarkable resemblance of humans and their virtual counterparts. The striking resemblance of humans and their corresponding avatars motivates us towards implementing a unique classification technique. This will not only help classify them but also serve as a tool to answer our previous question.

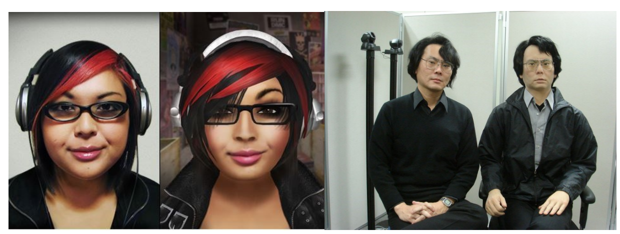

(a) (b)

Figure 1. Humans and their resembling avatars/robots. (a) Second Life avatar [13] (b) Geminoid - A humanoid designed by Hiroshi Ishiguro [14]

Our work addresses the goal of classifying natural (human) and artificial (avatar) faces. Two, unique, feature extracting techniques namely Uniform Local Directional Pattern (ULDP) and Wavelet Uniform Directional Pattern (WULDP) are applied on human and avatar face image datasets. Gaussian noise with zero mean and unit variance (default parameters) is applied to each image to measure the classifier's robustness. Chi-Square distance is used as the classifier. In ULDP, we select the uniform patterns (binary patterns with no more than two bitwise i.e. 0-

1 or 1-0 transitions) of Local Directional Pattern (LDP) which comparatively yield a smaller histogram as compared to the original LDP technique [15]. In WULDP, first-level decomposition using wavelet transforms (Daubechies Wavelet (db2) [16]) are applied on the images to acquire the approximation image. Next, ULDP is applied on this approximation image to achieve the classification accuracy. Experiments are conducted on two human datasets (Caltech and FERET) [17], [18] and three avatar datasets (Entropia, Second Life and Evolver) [19], [20].

II. Background and Related Work

The face is an instant and the most popular biometric used to classify or recognize individuals. Notable work has been carried out in applying biometric principles on avatar faces. *Artimetrics*: a field of study that identifies, classifies and authenticates avatars, virtual robots and virtual reality agents [9], verification and recognition of avatar faces [10], a personalized avatar creation system [21], Avatar DNA that aims to link the biometrics of the user to his/her avatar profile [22], detecting avatar faces [23], recognizing avatar faces [24] and examining the personality of an avatar's character based on its facial appearance [25]. Besides avatars, face recognition has also been applied on viewed sketches [26] and forensic sketches [27], [28] mapping them to their corresponding digital pictures. Local Binary Patterns (LBP) with varying neighborhood sizes [29], [30] and Wavelet transforms [31] have also been applied towards recognizing avatar faces. In general, complex neighborhoods in images have been described through advanced direction statistics before LBP and LDP. Dynamic Link Architecture in combination with Elastic Graph Matchingis used for object recognition [32]. Complex moments of Gabor power spectrum yield geometrically significant image attributes that are powerful texture descriptors [33].

A. Local Directional Pattern

Local Directional Pattern (LDP) uses the change in the gradient magnitude in a specific direction around the pixels to encode its local texture. Instead of comparing neighboring pixel intensities, it compares the neighboring pixel's gradient magnitude. It computes the edge response values in eight different directions and uses these to encode the image texture. This technique is robust in presence of noise and invariant to image rotations [15]. It assigns an eight bit binary code to each pixel of an input image by comparing the relative edge response value of that pixel in the eight different directions. Thus, eight directional edge response values of each pixel in eight different orientations are computed. Kirsch masks (Mask M_0 - Mask M_7) are used for this purpose centered on the pixel [34]. These masks are shown in Figure 2. Similar to LBP, the neighborhood size can always be extended to different sizes to accommodate representative features of certain types of textures.

$$\begin{bmatrix} -3 & -3 & 5 \\ -3 & 0 & 5 \\ -3 & -3 & 5 \end{bmatrix} \quad \begin{bmatrix} -3 & 5 & 5 \\ -3 & 0 & 5 \\ -3 & -3 & -3 \end{bmatrix} \quad \begin{bmatrix} 5 & 5 & 5 \\ -3 & 0 & -3 \\ -3 & -3 & -3 \end{bmatrix} \quad \begin{bmatrix} 5 & 5 & -3 \\ 5 & 0 & -3 \\ -3 & -3 & -3 \end{bmatrix}$$

East (Mask $\mathbf{M}_0$) **North East (Mask $\mathbf{M}_1$)** **North (Mask $\mathbf{M}_2$)** **North West (Mask $\mathbf{M}_3$)**

$$\begin{bmatrix} 5 & -3 & -3 \\ 5 & 0 & -3 \\ 5 & -3 & -3 \end{bmatrix} \quad \begin{bmatrix} -3 & -3 & -3 \\ 5 & 0 & -3 \\ 5 & 5 & -3 \end{bmatrix} \quad \begin{bmatrix} -3 & -3 & -3 \\ -3 & 0 & -3 \\ 5 & 5 & 5 \end{bmatrix} \quad \begin{bmatrix} -3 & -3 & -3 \\ -3 & 0 & 5 \\ -3 & 5 & 5 \end{bmatrix}$$

West (Mask $\mathbf{M}_4$) **South West (Mask $\mathbf{M}_5$)** **South (Mask $\mathbf{M}_6$)** **South East (Mask $\mathbf{M}_7$)**

Figure 2. Eight Kirsch edge response masks [15]

Applying each of these masks to a pixel we obtain its edge response values (m_0 - m_7), each representing the edge significance in eight directions. Response values are unequal in all directions. Presence of corners or edges yields high response values in particular directions. In order to generate the LDP, the *k* most prominent directions are determined. Thus, the top *k* values are set to 1 and the remaining (8-*k*) bits are set to 0. The equation for obtaining the LDP code is shown in (1).

$$LDP_k = \sum_{j=0}^{7} b_j (M_j - M_k) 2^j \tag{1}$$

where,

$$b_j(q) = \begin{cases} 1 & \text{if } q \geq 0 \\ 0 & \text{if } q < 0 \end{cases}$$

Figure 3 shows the mask response with the LDP bit positions and Figure 4 shows a sample LDP code with k=3.

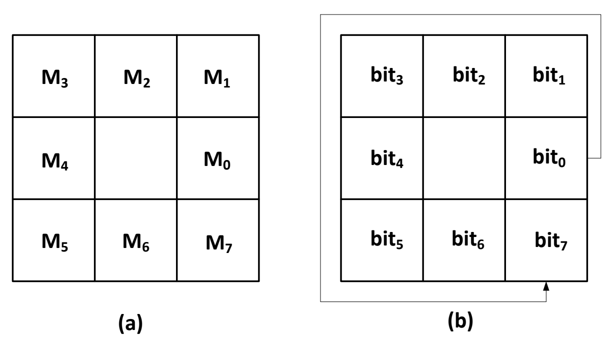

Figure 3. (a) Eight directional edge response positions based on the different mask positions. (b) Corresponding LDP binary bit positions [15].

B. Discrete Wavelet Transform on images

The Discrete Wavelet Transform (DWT) is a popular tool in image processing. It represents an image at lower

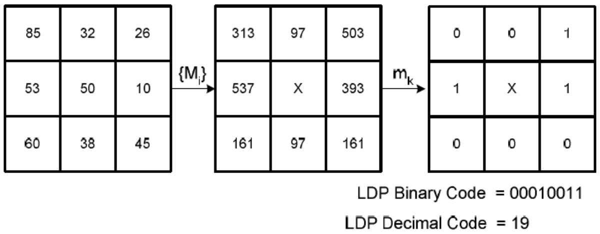

Figure 4. Sample LDP code with k=3 [15].

resolutions and provides the spatial and frequency characteristics of an image through multi-resolution analysis [24]. On applying 2D-DWT on an image, the first level wavelet decomposition provides four subbands, each having 1/2 resolution of the original image. Each subband represents the horizontal, vertical and diagonal edges of the image. An example is shown in Figure 5.

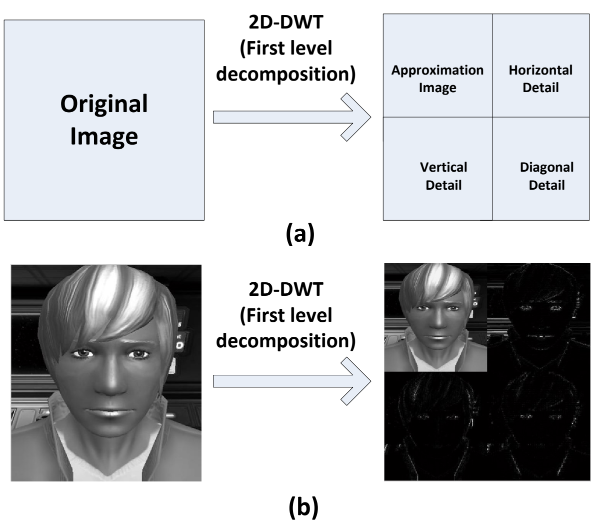

Figure 5. (a) First level decomposition after applying 2D-DWT (b) Applying the technique on a sample image.

C. Avatar CAPTCHA

CAPTCHAs (Completely Automated Public Turing Tests to Tell Computers and Humans Apart) aim to distinguish between human users and computer programs (bots) [35]. Besides text, there have been image CAPTCHAs designed as well. Avatar CAPTCHA is one such example [36]. Here the task is to identify images of avatars (artificial faces) from human faces from 12 grayscale images in each challenge. This is visually an easy task for human users to identify and solve whereas, it is a challenging task for a bot. Figure 6 shows an example of this CAPTCHA.

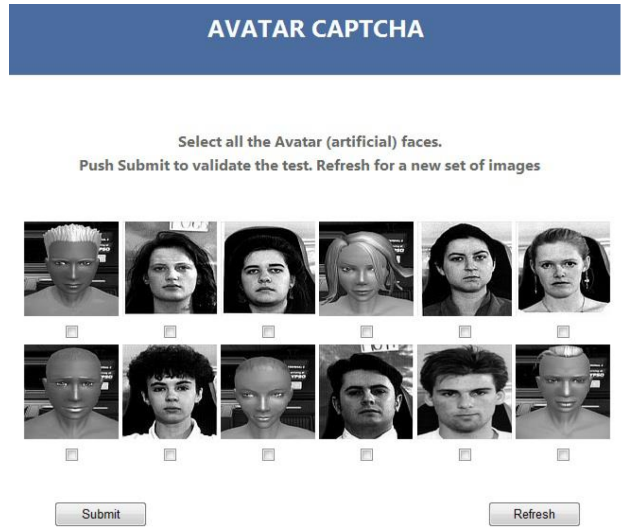

Figure 6. A snapshot of the Avatar CAPTCHA [36].

A challenge [37] was presented for this CAPTCHA to distinguish between human and avatar facial images. The goal of hosting this challenge was to determine how successful computer programs are at this task. A sample set of images is shown in Figure 7. There were some notable solutions that solved the problem fairly successfully [38]–[41].

Figure 7. A sample set of human and avatar facial images provided at the ICMLA Challenge 2012 [37].

Our work involves recognizing *uniform patterns* in the LDP patterns (k=3) and applying them towards classifying human and avatar facial images from different datasets to determine performance in terms of average accuracy, average training and test times. *Uniform patterns* refer to those patterns with no more than two binary bit transitions i.e. 0 to 1 or 1 to 0 in the circular presentation of the binary pattern. These patterns provide a vast majority of the examined texture patterns [42].

III. Experiment

We conducted two sets of experiments to obtain baseline results. *Experiment 1* involves applying ULDP on human and avatar face images and *Experiment 2* involves applying WULDP on the same set of images to obtain classification accuracies. The experiments were run on a Gateway desktop computer with an Intel core i7 processor with a clock frequency of 3.4 GHz, 10 GB DDR3 memory and 2 TB hard drive.

A. Datasets

Our datasets comprise of upright frontal faces with plain/non-plain backgrounds and varying illuminations. All images were 400 x 400 pixels in dimension. The datasets used were:

1) Humans: Set C - Caltech: Images from the California Institute of Technology [17] with non-plain backgrounds and varying illuminations.
Set F - FERET: Images from the FERET [18] dataset with plain backgrounds and varying illuminations.
Figure 8 shows sample images from the C and F datasets respectively.

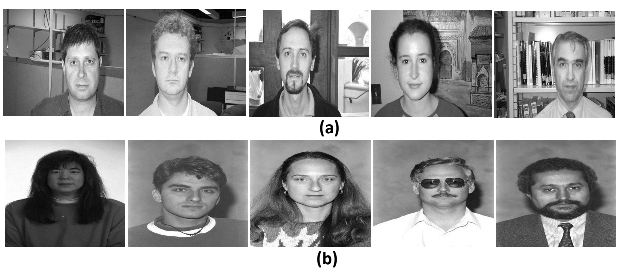

Figure 8. Sample human facial images from (a) Caltech (b) FERET datasets.

2) Avatars: Set E - Entropia Universe: Images obtained from a scripting technique designed to automatically collect avatar faces [19] with non-plain backgrounds.
Set SL - Second Life: Images obtained from the same scripting technique as that of Entropia [19] with non-plain backgrounds and varying illuminations.
Set EV - Evolver: Images from an automated bot, used to collect avatar images [20] with plain background and varying illuminations.
Figure 9 shows sample images from the E, SL and EV datasets respectively. Six human-avatar dataset combinations are used altogether: CE, CSL, CEV, FE, FSL, FEV. Each combination has a total of 300 images (150 human and 150 avatar images).

B. Uniform Local Directional Patterns (ULDP)

For *Experiment 1* we apply ULDP to classify the images from each dataset as a human or avatar. We consider the 8-neighbors for each pixel in the image. We obtain an 8-bit binary pattern i.e. values that range from 0-255. Of these, 56 values are LDP patterns with k=3. Of these 56 values, we obtain 8 uniform (8-bit binary patterns with no more than 2 bit transitions (0-1 or 1-0)) LDP values. These ULDP values obtained are 7, 14, 28, 56, 112, 131, 193 and 224. They are

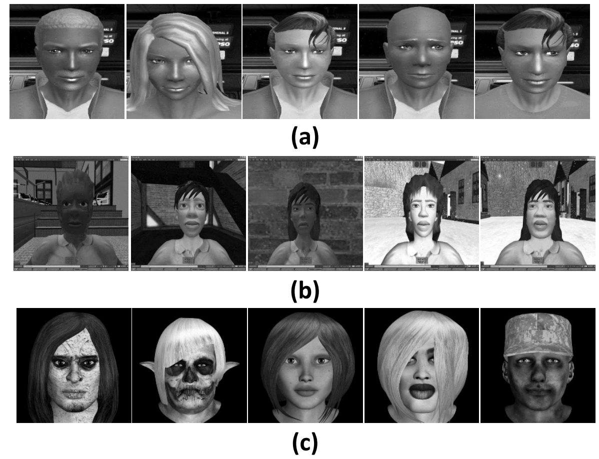

Figure 9. Sample avatar facial images from (a) Entropia Universe (b) Second Life (c) Evolver datasets.

used to create 8-bin histograms, reducing the feature vector dimension from 56 (for LDP) to 8 (for ULDP).

C. Applying ULDP over an image

First, we apply Gaussian noise with its default parameters (zero mean and unit variance) on all the images. This is done to test the robustness of the algorithm in presence of noise. Next, we subdivide each 400 x 400 image into regions of size 80 x 80. Thus, we end up with 25 regions per image. Next, we apply a 3 x 3 window with radius=1, neighbors=8 and threshold(k))=3 to each region to obtain the ULDP coded image using a mapping table. This table maps each ULDP value to a different bin and the remaining values to one single bin. Thus, we end up with a 7+1=8 bin local histogram for each region and a 25x8 bin histograms for the entire image. These histograms are concatenated to form a 1 x 200 bin global histogram which is the global descriptor for each image. Figure 10(a) shows the ULDP coded image generation process and Figure 11(a) shows the global descriptor generation process for an image.

D. Wavelet Uniform Local Directional Patterns (WULDP)

For *Experiment 2* we apply WULDP to classify the images from each dataset as a human or avatar. First, we apply the Gaussian noise with its default parameters (zero mean and unit variance) on all the images. Next, we perform first-level decomposition on the input noisy image through 2D discrete wavelet transform using Daubechies wavelet filter db2 [16] to obtain the approximation image. This approximation image has a resolution half of that of the original image i.e. 200 x 200. This speeds up its processing time. We subdivide each image into regions of size 40 x 40 thus, ending up with 25 regions per image. Finally, we apply the ULDP technique on this approximation image to obtain

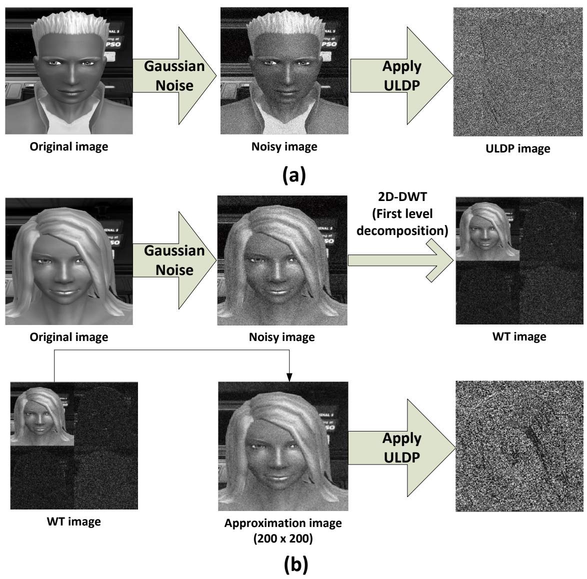

Figure 10. Coded image generation process (a) ULDP (b) WULDP.

the WULDP coded image. Figure 10(b) shows the WULDP coded image generation process and Figure 11(b) shows the global descriptor generation process for an image.

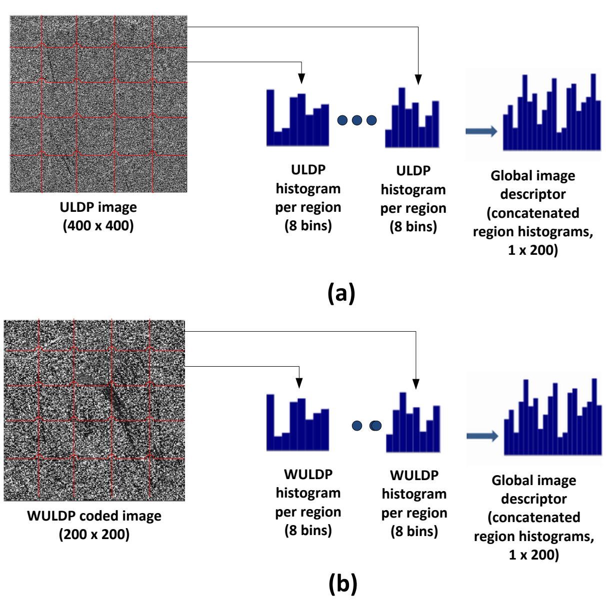

Figure 11. Global image descriptor generation (a) From ULDP coded image (b) From WULDP coded image.

For both experiments, a 10-fold cross validation is performed over each dataset. The training set comprises of 270 random images whereas the test set comprises of the remaining 30 images from the set. The Chi Square distance is used to classify the images yielding accuracies for each dataset. Training times, test times as well as accuracies for each fold are recorded. We report the average training times, test times as well as the overall accuracy for each dataset in the Results section below.

IV. Results

Results from *Experiment 1 (ULDP)* and *Experiment 2 (WULDP)* for each dataset are presented in Table I and Table II respectively with the average values over 10 folds of cross-validation.

Table I
RESULTS OVER 10 FOLDS OF CROSS-VALIDATION FOR EACH DATASET FOR *Experiment 1*. IMAGE RESOLUTION = 400 X 400, WINDOW SIZE = 3 X 3, RADIUS=1, NEIGHBORS = 8, REGION SIZE = 80 X 80.

Datasets	**Avg. Training Time (secs)**	**Avg.Test Time (secs)**	**Overall Accuracy (%)**
CE	45.97	45.87	99
CSL	49.07	48.49	95
CEV	47.46	47.03	100
FE	47.21	47.24	100
FSL	48.21	48.28	97.33
FEV	51.91	48.66	100
Overall average	48.30	47.59	98.55

From Table I we observe that for *Experiment 1*, best accuracies are achieved for the CEV, FE and FEV datasets. The EV and the F datasets have plain backgrounds which provide distinct patterns for classification. However, when evaluated against each other the results are remarkable which demonstrates the power of the ULDP descriptor. Executing this experiment on the entire image yields higher average training and testing times as that in *Experiment 2*.

Table II
RESULTS OVER 10 FOLDS OF CROSS-VALIDATION FOR EACH DATASET FOR *Experiment 2*. IMAGE RESOLUTION = 200 X 200, WINDOW SIZE = 3 X 3, RADIUS = 1, NEIGHBORS = 8, REGION SIZE = 40 X 40.

Datasets	**Avg. Training Time (secs)**	**Avg.Test Time (secs)**	**Overall Accuracy (%)**
CE	11.18	11.16	82.67
CSL	11.07	11.08	87.33
CEV	11.66	11.57	94.67
FE	11.37	11.46	87.33
FSL	11.66	11.55	96.33
FEV	12.15	12.17	89
Overall average	11.51	11.49	89.55

From Table II we observe that for *Experiment 2*, good accuracies are achieved for the FSL and CEV datasets. Since this experiment is executed on the approximate image it yields lower average training and testing times.

Figure 12 shows the ROC curves for both sets of experiments. The ULDP curves are segregated into three parts for clarity. Overall, we observe that ULDP descriptors are better than WULDP in classifying human and avatar facial images.

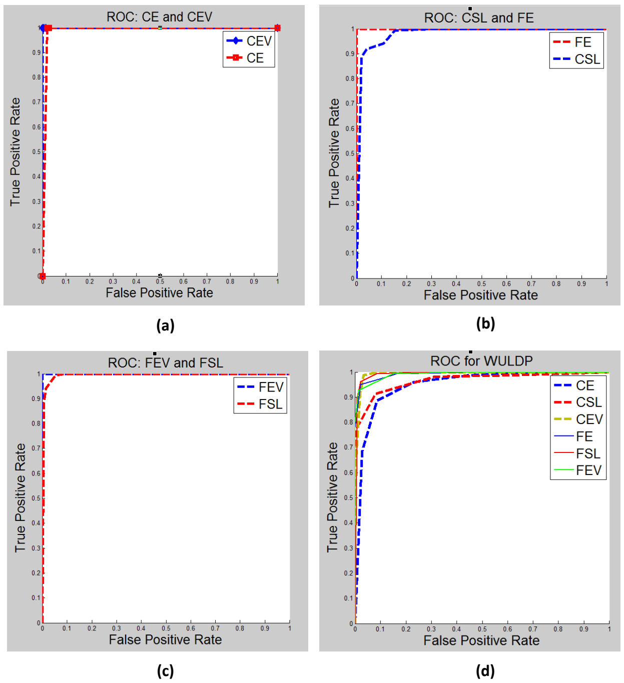

Figure 12. ROC curves for *Experiment 1: ULDP* (a) CE and CEV (b) CSL and FE (c) FEV and FSL (d) *Experiment 2: WULDP*.

V. Conclusions and Future Work

Our work involves the classification of natural and artificial faces. To address this we have implemented two techniques, namely ULDP and WULDP and applied them on human (natural) and avatar (artificial) datasets to classify them in the presence of Gaussian noise. Our experiments report good baseline results. The accuracy rates achieved in ULDP are higher than WULDP suggesting that uniform patterns obtained from the original image are much better descriptors than those obtained from the approximate image after wavelet transform. We intend to expand our work by using different datasets, utilizing uniform patterns with different thresholds (k-value) and varying noise intensity levels over the images to help achieve comparable results.

References

[1] T. R. Kalansuriya and A. T. Dharmaratne, "Facial image Classification based on Age and Gender," in *International Conference on Advances in ICT for Emerging Regions (ICTer)*. Colombo, Sri Lanka: IEEE, 2013, pp. 44–50.

[2] Y. H. Kwon and N. da Vitoria Lobo, "Age Classification from Facial Images," in *IEEE Computer Society Conference on Computer Vision and Pattern Recognition*, Seattle, Washington, USA, 1994, pp. 762–767.

[3] C. BenAbdelkader and P. Griffin, "A local region-based approach to gender classification from face images," in *IEEE Computer Society Conference on Computer Vision and Pattern Recognition-Workshops*, San Diego, California, USA, June, 2005, pp. 52–52.

[4] C. Shan, "Learning Local Binary Patterns for Gender Classification on Real-world Face Images," *Pattern Recognition Letters*, vol. 33, no. 4, pp. 431–437, 2012.

[5] Z. Hammal, L. Couvreur, A. Caplier, and M. Rombaut, "Facial expression classification: An approach based on the fusion of Facial Deformations using the Transferable Belief model," *International Journal of Approximate Reasoning*, vol. 46, no. 3, pp. 542–567, 2007.

[6] M. Liang, Y. Zhuang, and C. Cai, "Face Classification using Sparse Reconstruction Embedding," in *International Conference on Computational Intelligence and Software Engineering (CiSE)*, Wuhan, China, 2010, pp. 1–4.

[7] A. S. Irwin, J. Slay, K.-K. R. Choo, and L. Lui, "Money Laundering and Terrorism Financing in Virtual Environments: A feasibility study," *Journal of Money Laundering Control*, vol. 17, no. 1, pp. 50–75, 2014.

[8] M. R. Lyu, I. King, T. Wong, E. Yau, and P. Chan, "ARCADE: Augmented Reality Computing Arena for Digital Entertainment," in *Aerospace Conference*. Big Sky, Montana, USA: IEEE, 2005, pp. 1–9.

[9] R. V. Yampolskiy and M. L. Gavrilova, "Artimetrics: Biometrics for Artificial Entities," *Robotics & Automation Magazine, IEEE*, vol. 19, no. 4, pp. 48–58, 2012.

[10] R. V. Yampolskiy, B. Klare, and A. K. Jain, "Face Recognition in the Virtual World: Recognizing Avatar faces," in *11th International Conference on Machine Learning and Applications (ICMLA)*, vol. 1. Boca Raton, Florida, USA: IEEE, 2012, pp. 40–45.

[11] M. Dyck, M. Winbeck, S. Leiberg, Y. Chen, R. C. Gur, and K. Mathiak, "Recognition profile of emotions in natural and virtual faces," *PLoS One*, vol. 3, no. 11, p. e3628, 2008.

[12] Cleverbot and Cleverscript, "Evie: The Avatar Chatbot," http://www.existor.com.

[13] "Second Life," http://www.secondlife.com.

[14] S. Nishio, H. Ishiguro, and N. Hagita, "Geminoid: Teleoperated Android of an existing person," *Humanoid robots-new developments. I-Tech*, vol. 14, 2007.

[15] T. Jabid, M. H. Kabir, and O. Chae, "Local Directional Pattern (LDP) - A Robust Image Descriptor for Object Recognition," in *Proc. 7th IEEE International Conference on Advanced Video and Signal Based Surveillance*. Boston, Massachussets, USA: IEEE Computer Society, 2010, pp. 482–487.

[16] I. Daubechies, "The wavelet transform, time-frequency localization and signal analysis," *IEEE Trans. on Inf. Theory*, vol. 36, no. 5, pp. 961–1005, 1990.

[17] M. Weber, "A Frontal face dataset collected by Markus Weber at the California Institute of Technology," http://www.vision.caltech.edu/Image_Datasets/faces, 1999.

[18] P. Phillips, "The Facial Recognition Technology (FERET) Database," *IEEE Transactions on Pattern Analysis and Machine Intelligence*, vol. 22, 2004.

[19] J. N. Oursler, M. Price, and R. V. Yampolskiy, "Parameterized generation of Avatar Face Dataset," in *14th International Conference on Computer Games: AI, Animation, Mobile, Interactive Multimedia, Educational & Serious Games*, Louisville, Kentucky, USA, 2009, pp. 17–22.

[20] J. Kim, D. D'Souza, and R. V. Yampolskiy, "Automated Collection of High Quality 3D Avatar images," in *Proc. 23rd Midwest Artificial Intelligence and Cognitive Science*, vol. 841, Cincinnati, Ohio, USA, 2012, p. 78.

[21] M. Lyons, A. Plante, S. Jehan, S. Inoue, and S. Akamatsu, "Avatar Creation using Automatic Face Processing," in *Proceedings of the Sixth ACM international conference on Multimedia*, Bristol, UK, 1998, pp. 427–434.

[22] R. Yampolskiy and M. Gavrilova, "Applying Biometric Principles to Avatar Recognition," in *Proc. International Conference on Cyberworlds (CW2010)*, A. Sourin and O. Sourina, Eds., Singapore, 2010, pp. 179–186.

[23] D. D'Souza and R. Yampolskiy, "Baseline Avatar Face Detection using an Extended set of Haar-like features," in *Midwest Artificial Intelligence and Cognitive Science Conference*, Cincinnati, Ohio, USA, April, 2012, p. 72.

[24] A. Mohamed and R. V. Yampolskiy, "Face Recognition based on Wavelet Transform and Adaptive Local Binary Pattern," in *Digital Forensics and Cyber Crime*. Springer, 2013, vol. 114, pp. 158–166.

[25] W. Yuqiong, J. Geigel, and A. Herbert, "Reading Personality: Avatar vs. Human Faces," in *Humaine Association Conference on Affective Computing and Intelligent Interaction (ACII)*, Geneva, Switzerland, 2013, pp. 479–484.

[26] X. Wang and X. Tang, "Face photo-sketch synthesis and recognition," *IEEE Transactions on Pattern Analysis and Machine Intelligence*, vol. 31, no. 11, pp. 1955–1967, 2009.

[27] B. F. Klare, Z. Li, and A. K. Jain, "Matching forensic sketches to mug shot photos," *IEEE Transactions on Pattern Analysis and Machine Intelligence*, vol. 33, no. 3, pp. 639–646, 2011.

[28] B. Klare and A. K. Jain, "Sketch-to-photo matching: a feature-based approach," in *SPIE Defense, Security, and Sensing*. Orlando, Florida, USA: International Society for Optics and Photonics, 2010, pp. 766 702–766 702–10.

[29] A. A. Mohamed and R. V. Yampolskiy, "An improved LBP algorithm for avatar face recognition," in *XXIII International Symposium on Information, Communication and Automation Technologies (ICAT)*. Sarajevo, Bosnia and Herzegovina: IEEE, 2011, pp. 1–5.

[30] A. A. Mohamed, D. D'Souza, N. Baili, and R. V. Yampolskiy, "Avatar face recognition using wavelet transform and hierarchical multi-scale LBP," in *10th International Conference on Machine Learning and Applications and Workshops (ICMLA)*, vol. 1. Honolulu, Hawaii, USA: IEEE, 2011, pp. 194–199.

[31] A. A. Mohamed, M. L. Gavrilova, and R. V. Yampolskiy, "Recognizing avatar faces using wavelet-based adaptive local binary patterns with directional statistical features," in *Transactions on Computational Science XVIII*. Springer, 2013, vol. 7848, pp. 137–154.

[32] M. Lades, J. Vorbruggen, J. Buhmann, J. Lange, C. v. d. Malsburg, R. P. Hurtz, and W. Konen, "Distortion invariant object recognition in the dynamic link architectures," *IEEE Trans. on Computers*, vol. 42, no. 3, pp. 300–311, 1993.

[33] J. Bigun and J. du Buf, "N-folded symmetries by complex moments in Gabor space," *pami*, vol. 16, no. 1, pp. 80–87, 1994.

[34] T. Jabid, M. Kabir, and O. Chae, "Local Directional Pattern (LDP) for Face Recognition," in *Digest of Technical Papers, International Conference on Consumer Electronics (ICCE)*, Las Vegas, Nevada, USA, 2010, pp. 329–330.

[35] L. V. Ahn, M. Blum, and J. Langford, "The Captcha Project," http://www.captcha.net.

[36] D. D'Souza, P. C. Polina, and R. V. Yampolskiy, "Avatar CAPTCHA: Telling computers and humans apart via face classification," in *Proc. 2012 IEEE International Conference on Electro/Information Technology (EIT)*, Indianapolis, Indiana, USA, May, 2012, pp. 1–6.

[37] R. V. Yampolskiy and D. D'Souza, "ICMLA Face Recognition challenge," http://www.icmla-conference.org/icmla12/.

[38] T. Yamasaki and T. Chen, "Face Recognition challenge: Object Recognition approaches for Human/Avatar Classification," in *11th International Conference on Machine Learning and Applications (ICMLA)*, vol. 2. Boca Raton, Florida, USA: IEEE, 2012, pp. 574–579.

[39] B. Cheung, "Convolutional Neural Networks applied to Human Face Classification," in *11th International Conference on Machine Learning and Applications (ICMLA)*, vol. 2. Boca Raton, Florida, USA: IEEE, 2012, pp. 580–583.

[40] M. Korayem, A. A. Mohamed, D. Crandall, and R. V. Yampolskiy, "Learning Visual Features for the Avatar Captcha Recognition challenge," in *11th International Conference on Machine Learning and Applications (ICMLA)*, vol. 2. Boca Raton, Florida, USA: IEEE, 2012, pp. 584–587.

[41] S. Alelyani and H. Liu, "Ensemble Feature Selection in Face Recognition: ICMLA 2012 Challenge," in *11th International Conference on Machine Learning and Applications (ICMLA)*, vol. 2. Boca Raton, Florida, USA: IEEE, 2012, pp. 588–591.

[42] T. Ojala, M. Pietikainen, and T. Maenpaa, "Multiresolution Gray-scale and Rotation invariant Texture Classification with Local Binary Patterns," *IEEE Transactions on Pattern Analysis and Machine Intelligence*, vol. 24, no. 7, pp. 971–987, 2002.